Benign Disease of the Uterus

3

Karen Kinkel, Susan M. Ascher, and Caroline Reinhold

Learning Objectives

- To be able to identify and classify Müllerian anomalies and leiomyomas with ultrasound and MRI
- To diagnose adenomyosis, deep endometriosis, and complicated leiomyomas
- To differentiate endometrial polyps from submucosal leiomyoma

Key Points

- The diagnosis of Müllerian anomalies takes into account the uterine shape, external contour, and width of internal indentation compared to the uterine wall thickness. Associated anomalies of the cervix or vagina are classified separately.
- Classification of leiomyomas indicates how far the myometrial anomalies traverse the interface between the endometrial/myometrial interface and the myometrial/serosal interface. Analysis of T2-, T1-, and diffusion-weighted signal intensity and contrast enhancement helps in determining treatment strategies in symptomatic patients.

K. Kinkel (✉)
Institut de radiologie, Clinique des Grangettes, Chêne-Bougeries, Geneva, Switzerland
e-mail: Karen.kinkel@grangettes.ch

S. M. Ascher
Department of Radiology, Georgetown University School of Medicine, Washington, DC, USA
e-mail: aschers@gunet.georgetown.edu

C. Reinhold
Department of Radiology, McGill University Health Center, Montreal, QC, Canada
e-mail: Caroline.reinhold@mcgill.ca

3.1 Introduction

Endovaginal sonography (EVS) is the procedure of choice for the initial evaluation of benign diseases of the female genital tract. When EVS findings are indeterminate, further evaluation is often performed with magnetic resonance imaging (MRI) due to its excellent soft tissue differentiation, multiplanar capabilities, and absence of ionizing radiation. MRI is used as a problem-solving tool in benign uterine diseases, for example, uterine malformations, adenomyosis, and deep endometriosis, and to select appropriate candidates for therapies such as myomectomy or different types of hysterectomy. The role of computed tomography (CT) is limited in the evaluation of benign disease of the female pelvis particularly due to its lack of soft tissue differentiation. CT is primarily employed in an emergency situation, such as in an acute abdomen caused by ovarian torsion or pelvic inflammatory disease.

3.2 Normal Anatomy of the Uterus

In women of reproductive age, the uterus is approximately 6–9 cm in length and varies in appearance according to the menstrual cycle. On EVS, the thickness of the endometrium in premenopausal women increases progressively during the menstrual cycle: from 3 to 8 mm in the proliferative phase to 8–12 mm or more in the secretory phase. The echotexture of the endometrium also varies. The endometrium is hypo- to isoechoic in the mid-proliferative phase and becomes trilaminar in the periovulatory phase. In the secretory phase, the endometrium becomes echogenic and may have a nodular appearance. In the inner myometrium, subjacent to the endometrium, a thin hypoechoic line is visible called the subendometrial halo. This line does not correspond anatomically to the junctional zone on MRI and is typically thinner. The remainder of the myometrium is of intermediate

J. Hodler et al. (eds.), *Diseases of the Abdomen and Pelvis 2018–2021*, IDKD Springer Series,
https://doi.org/10.1007/978-3-319-75019-4_3

echogenicity. Sonographic studies of endometrial thickness in postmenopausal women have suggested an upper limit of 5 mm in patients not on hormone replacement and 8 mm for patients receiving hormonal therapy. EVS is highly sensitive for detecting endometrial pathology when these cutoff values are used as guidelines, to determine which patients would benefit from endometrial sampling [1]. The presence of endometrial thickening on EVS is nonspecific and may be due to endometrial hyperplasia, polyps, or carcinoma. The uterine zonal anatomy on MRI is best depicted using sagittal T2-weighted images (Fig. 3.1).

In the premenopausal woman, the high signal intensity endometrium varies in thickness, depending on the menstrual cycle. In postmenopausal patients, the uterine corpus, but not the cervix, decreases in size. On dynamic gadolinium-enhanced images, the endometrium is hypovascular relative to the myometrium and becomes iso- or hyperintense on delayed scans.

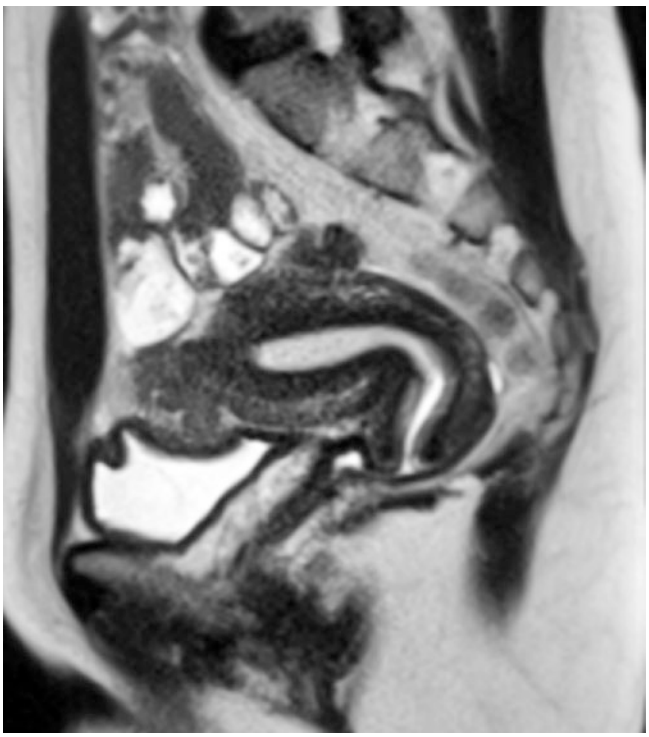

Fig. 3.1 Normal MRI Uterine Anatomy Sagittal 3D T2-weighted multiplanar reconstruction of the uterus and cervix demonstrates normal zonal anatomy. There are three zones identifiable in the uterus: the hyperintense endometrium, the hypointense junctional zone and the intermediate signal intensity of the outer myometrium. Four zones are distinguished in the cervix: the hyperintense mucous within the endocervical canal, the intermediate signal intensity of the cervical mucosa, the hypointense cervical stroma, and the intermediate signal intensity of the outer smooth muscle

3.3 MRI Technique

Patient preparation is an important step to obtain optimal image quality. To minimize motion artifacts due to bowel motion, patients are asked to fast 6 h prior to imaging. Unless contraindicated, intravenous or intramuscular injection of peristaltic inhibitors, i.e., glucagon or butyl-scopolamine, is recommended to further decrease peristalsis artifacts. According to the clinical question, additional preparation might include bowel cleansing and/or vaginal opacification for chronic pelvic pain. Sonographic gel is used to opacify the vagina and to allow visualization of vaginal duplication or communication. An intravenous line is often required to inject contrast agent to determine vascularity of myometrial or endocavitary abnormalities. Examinations are usually performed in supine position using a body-flex phased-array MR surface coil. Imaging of the uterus should be performed using the smallest possible field of view (20–24 cm), thin sections of 3.5–4 mm, and the largest possible matrix size appropriate to each individual sequence. These imaging parameters provide important anatomic detail, which becomes critical when imaging uterine anomalies and endometrial pathology. When imaging large leiomyomas, the section thickness and field of view (FOV) may need to be adjusted accordingly. However, when establishing the myometrial origin of a subserosal leiomyoma, thin sections at the level of the pedicle are frequently helpful.

The most important sequence is a T2-weighted sequence nicely demonstrating the zonal anatomy of the uterus. Sagittal sections are best suited to image the uterus. Oblique coronal and axial slice orientation according to the long and short axis of the endometrial cavity should be applied for the assessment of uterine and cervical pathologies. It is important to train MR technologists on how to acquire these oblique sequences if physician supervision is not possible. The short-axis coronal oblique sequence (perpendicular to the long axis of the endometrial cavity) is particularly valuable for assessing localized endometrial pathology and for evaluating the thickness of the junctional zone. It is also valuable for determining the extent of a uterine septum. A T2-weighted sequence performed parallel to the long axis of the endometrial cavity is critical to characterize the external uterine contour in patients with Müllerian duct anomalies. Since this series is so important in the classification of uterine anomalies, it is best performed earlier in the examination, prior to bladder filling, which often displaces the uterus as it becomes increasingly distended. If the fundal contour is inadequately characterized by the T2-weighted images, T1-weighted images parallel to the long axis can facilitate

characterization of the external contour due to increased contrast between the myometrial fundal contour and the overlying fat. Recent software advances allow for a 3D T2-weighted acquisition—allowing post-processing of the uterus in any plane and potentially obviating the need to acquire individual orthogonal 2D T2-weighted sequences.

In addition to T2-weighted sequences, T1-weighted sequences with and without fat suppression are helpful to distinguish bloody components in adenomyosis or potential sarcomas from fat or mucinous components. A T1-weighted 3D Dixon gradient echo sequence allows for T1-weighted in-phase, T1-weighted out-of-phase, T1-weighted water excitation, and T1-weighted fat excitation images within a single breath-hold. Routine use of this sequence helps standardize imaging protocols without additional exam time. In patients with congenital anomalies, a quick breath-hold T1-weighted sequence covering both kidneys is helpful to exclude renal agenesis or hydronephrosis.

An axial echo-planar diffusion-weighted imaging (DWI) sequence is an increasingly helpful functional imaging technique whose contrast derives from the random motion of water molecules within the extracellular tissue. In specific situation, such as patients with a leiomyoma of intermediate T2-weighted signal intensity, the high signal intensity of the DWI sequence combined with low or heterogeneous T1 signal intensity has the potential to differentiate leiomyomas from sarcomas or indeterminate myometrial masses with the use of an apparent diffusion coefficient (ADC) [2]. However measuring ADCs in all leiomyoma regardless T2 or DWI signal intensity is of no value and wrongly increases the rate of suspicion.

Gadolinium-enhanced imaging is not needed for most benign conditions, but can be useful in selected pathologies. We routinely perform contrast-enhanced imaging in patients referred for evaluation of endometrial pathology. In addition, contrast-enhanced imaging is also performed in patients with symptomatic leiomyomas scheduled for laparoscopic surgery or uterine artery embolization, in the latter case with additional MR angiography of the iliac arteries. Vascularity can help to predict response to treatment, and the enhancement may help distinguish a benign fibroid from a malignant leiomyosarcoma.

3.4 Congenital Anomalies

Between the 6th and 11th weeks of gestation, the paired Müllerian ducts undergo descent, fusion, and septum resorption to form the uterus, fallopian tubes, cervix, and upper 2/3 of the vagina [3]. Müllerian duct anomalies (MDAs) result when this process either fails or is interrupted. Depending on the anomaly, patients may be asymptomatic with normal fertility and obstetric outcomes, while others may have primary amenorrhea, menstrual irregularities, infertility, obstetric complications, and/or endometriosis. The reported prevalence of MDAs varies widely: 1–5% in the general population and 13–25% in women with recurrent fetal loss [4]. The ovaries and external genitalia/distal 1/3 of the vagina are spared because they originate from the primitive yolk sac and sinovaginal bud, respectively. Renal anomalies however are present in 30–50% of women with MDAs [5].

Appropriate classification is critical to ensure proper treatment. Buttram and Gibbons classified MDAs in 1979, and a revised classification by the American Society for Reproductive Medicine (formerly the American Fertility Society) was published in 1988 [6, 7]**.** While widely accepted, the AFS system had limitations "in terms of effective characterization of anomalies, clinical usefulness, simplicity and friendliness" [8]. To address these limitations, the European Society of Human Reproduction and Embryology (ESHRE) and the European Society for Gynaecological Endoscopy (ESHE) established a working group to develop a new updated classification system that would be more clinically oriented and based on anatomy. The group published their consensus classification of female genital tract congenital anomalies in 2013. The ESHRE/ESGE system sorts anomalies into classes and subclasses based on increasing severity of anatomical deviation, from normal (U0) to unclassified cases (U6) (Fig. 3.2).

Use of absolute numbers to define an anomaly was discarded; rather, the new system defines uterine deformity in relation to anatomical landmarks, for example, uterine wall thickness (UWT) which is defined as the distance between the interostial line and a parallel line on the top of the fundus [9].

When a MDA is suspected, US is the most commonly performed exam and may be diagnostic, especially if a 3D US is performed (Fig. 3.3). However, MRI remains the preferred imaging technique in patients where TVS is not possible due to vaginal agenesis, in patients with complex uterine anomalies, or in diagnostic dilemmas [9]. MRI has been shown in multiple studies to have excellent agreement with MDA subtype classifications [10].

3.4.1 Class 0 (Normal Uterus)

The normal uterus is defined as having either a straight or curved interostial line with an internal indentation $\leq 50\%$ of the UWT at the fundal midline (Figs. 3.2, 3.3, 3.4, 3.5, 3.6, 3.7, 3.8, 3.9, 3.10, 3.11 and 3.12).

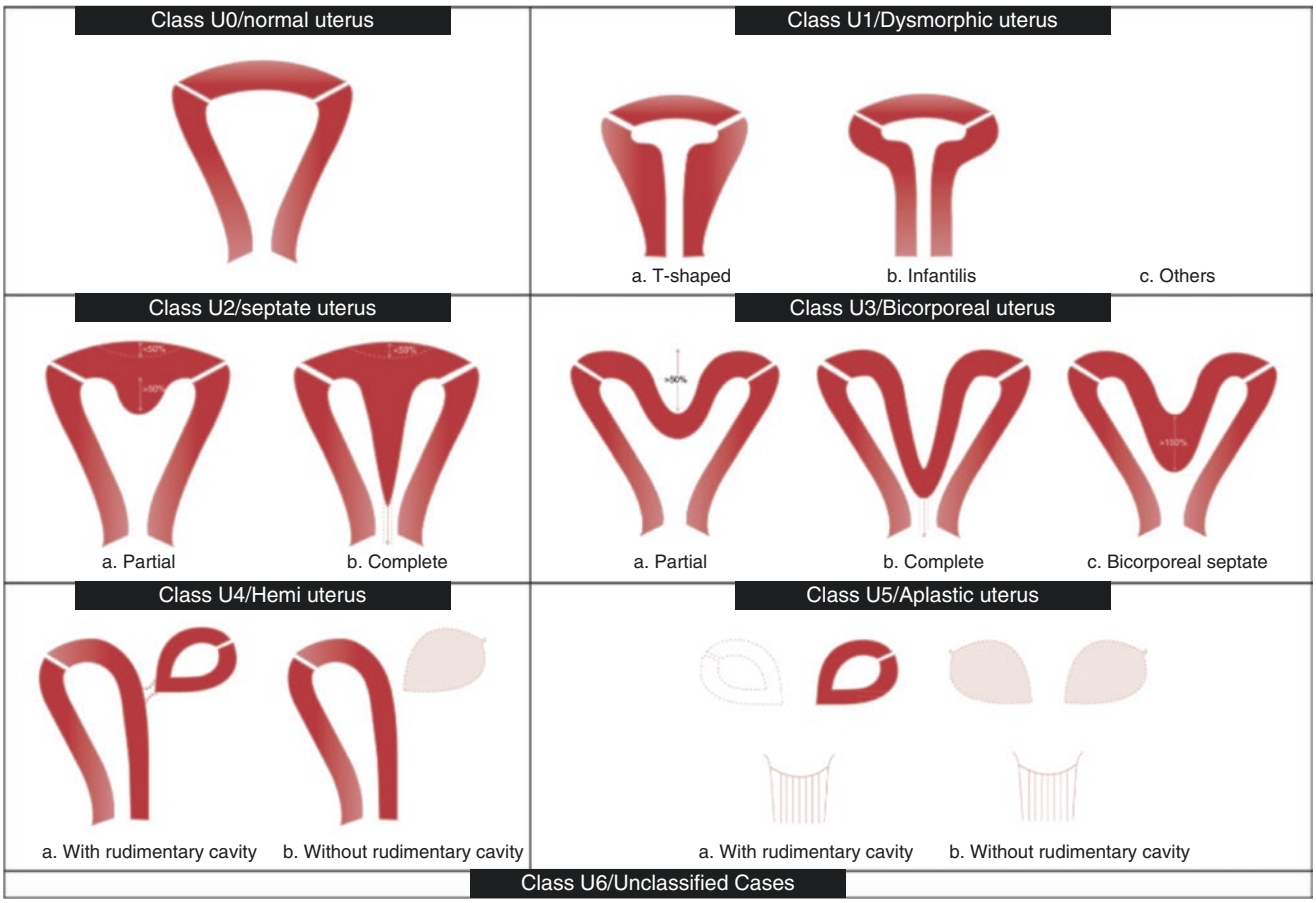

Fig. 3.2 Schematic drawing of the ESHRE/ESGE classification system of uterine congenital anomalies from Ref. [8], dividing uterine anomalies in six classes

3.4.2 Class U1 (Dysmorphic Uterus)

This category encompasses uteri with a normal uterine outline that have an abnormal cavity excluding septa. U1 anomalies have three subtypes:

1. U1a (T-Shaped Uterus)—narrow uterine cavity with thickened lateral walls with a normal corpus-to-cervix ratio
2. U1b (Uterus Infantilis)—narrow uterine cavity with normal lateral walls with an abnormal corpus-to-cervix ratio
3. U1c (Others)—all other minor deformities of the uterine cavity with a midline, fundal, inner indentation <50% UWT

3.4.3 Class U2 (Septate Uterus) (Fig. 3.4)

This category reflects abnormal resorption of the midline septum following normal Müllerian duct fusion. The uterus has a normal outer contour, but the midline, fundal, inner indentation is >50% of the UWT. U2 anomalies have two subtypes:

1. U2a (Partial Septate)—midline fundal inner septum divides the uterine cavity above the internal os.
2. U2b (Complete Septate)—midline fundal inner septum divides the uterine cavity up to the internal os. There may be associated cervical or vaginal anomalies. Fig. 3.4. MRI of the pelvis: T2-weighted axial-oblique image (coronal plane of the uterine cavity) demonstrates a complete hypointense septum through the entire length of the hyperintense uterine cavity.

The composition of the septum is variable and is often myometrial proximally and more fibrous distally [11, 12]. Fetal wastage is common in these women with a spontaneous abortion rate of 65%. Treatment reflects the makeup of the septum. If the septum is primarily fibrous, a hysteroscopic septoplasty can be performed with good results. If, however, the septum is primarily myometrial, a combined laparoscopic-hysteroscopic surgical approach is warranted [13].

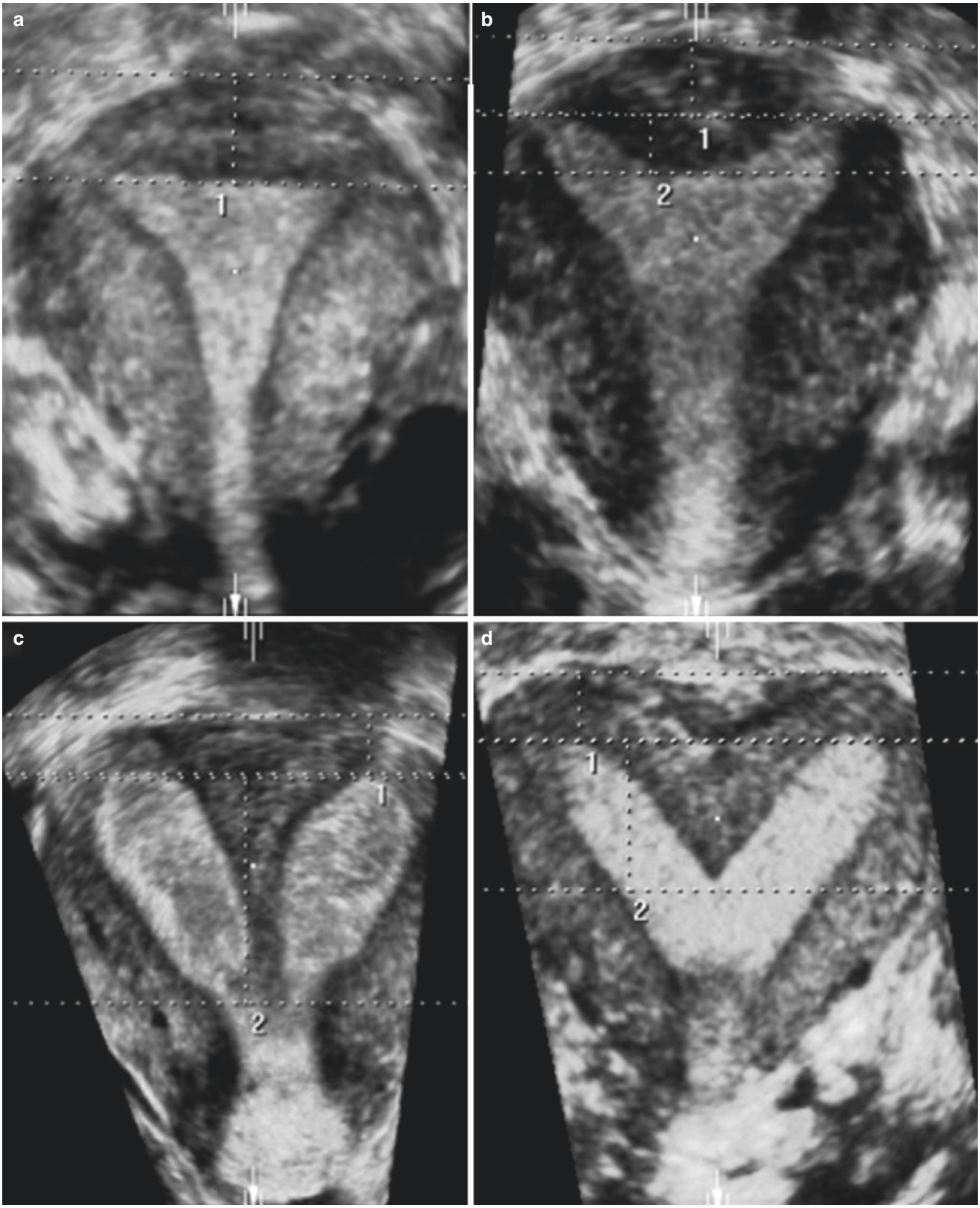

Fig. 3.3 Ultrasound images of the uterus in a coronal plane of the uterine cavity (modified from Ref. [9], demonstrate how to measure the uterine wall thickness (1) as well as the length of the internal midline indentation (2) for a normal uterus (**a**), a partial septate uterus (**b**), a complete septate uterus (**c**) and a bicorporal uterus (**d**)

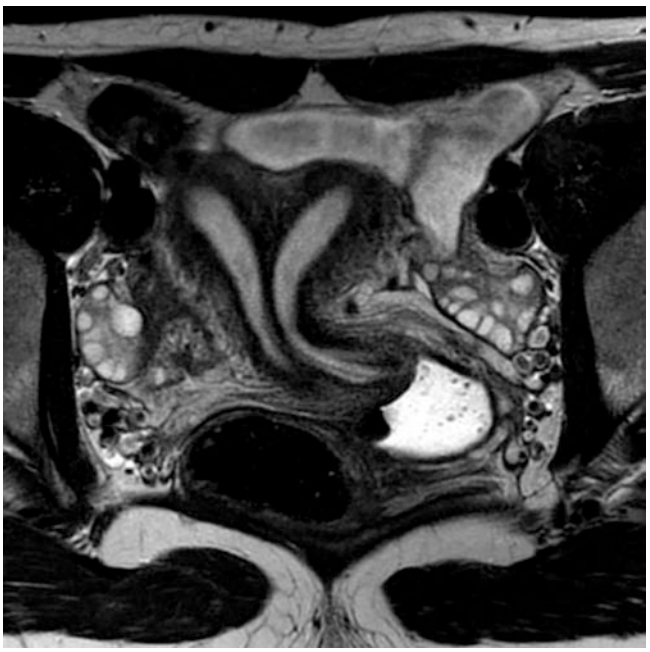

Fig. 3.4 MRI of the pelvis: T2-weighted axial-oblique image (coronal plane of the uterine cavity) demonstrates a complete hypointense septum through the entire length of the hyperintense uterine cavity

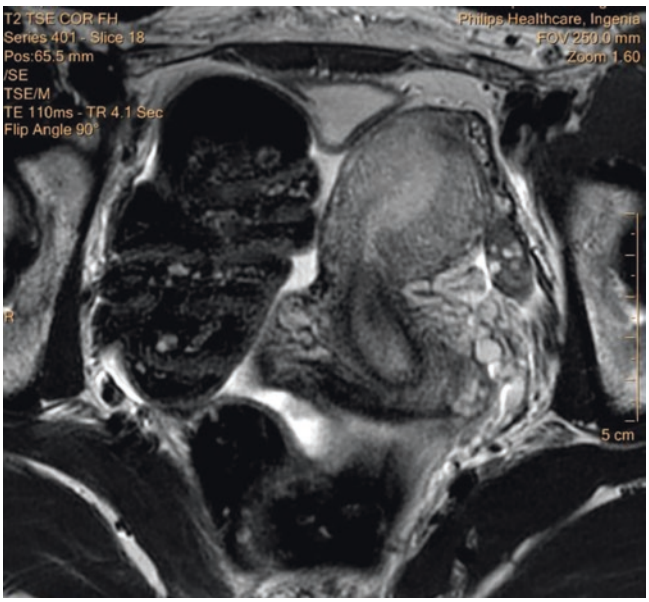

Fig. 3.6 MRI of the pelvis: T2-weighted axial image through the coronal plane of a "banana"—shaped left hemi-uterus without evidence of a rudimentary remnant uterine horn

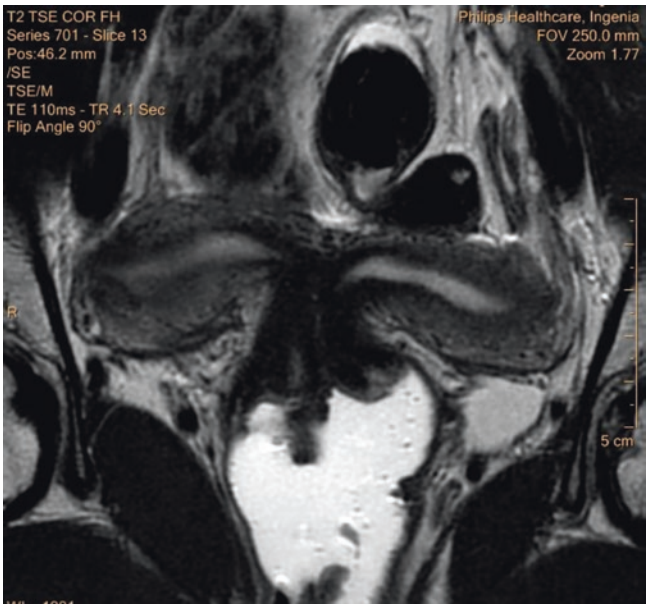

Fig. 3.5 MRI of the pelvis: T2-weighted coronal image through the coronal plane of the uterine cavity of the bicorporeal complete uterus with an associated double normal cervix (C2). Opacification of the vagina with sonographic gel helps to exclude vaginal septa

Fig. 3.7 MRI of the pelvis: T2-weighted coronal oblique view of the uterine cavity shows a type 1 submucosal leiomyoma with more than 50% of the volume inside the uterine cavity. A second leiomyoma lies in close contact to the endometrium (class 3 of an intra-mural leiomyoma)

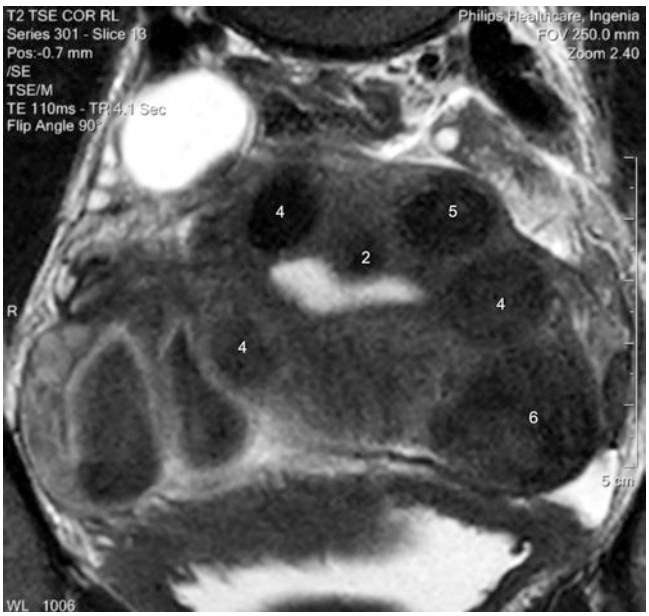

Fig. 3.8 MRI of the pelvis T2-weighted coronal image (axial oblique orientation of the uterus) with type 3, 4, 5 and 6 leiomymoma

3.4.4 Class U3 (Bicorporeal Uterus, syn: Bicornuate Uterus) (Fig. 3.5)

This category is a result of abnormal fusion of Müllerian ducts. The uterus will have an abnormal fundal contour with an external indentation at the fundal midline >50% of the UWT. U3 anomalies have three subtypes:

1. U3a (Partial Bicorporeal Uterus)—external fundal indentation divides the uterus above the internal os.
2. U3b (Complete Bicorporeal Uterus)—external fundal indentation divides the uterus to the internal os. There may be associated cervical and/or vaginal anomalies.
3. U3c (Bicorporeal Septate Uterus)—the width of the midline inner fundal indentation >150% of the UWT.

Vaginal or hysteroscopic septoplasty is reserved for patients with an obstructing vaginal septum (U3b) or septate form of the anomaly (U3c), respectively.

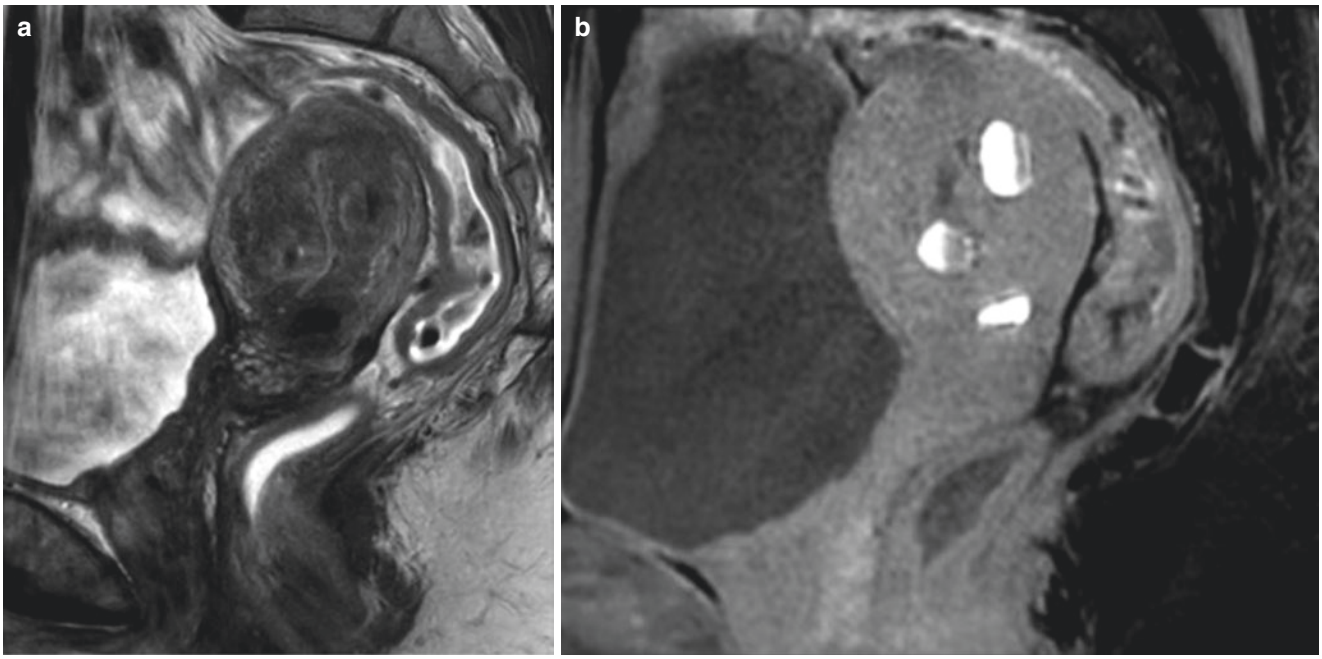

Fig. 3.9 (**a**) MRI of the pelvis T2-weighted sagittal image through the mid uterine body: a thickened junctional zone is associated with two cystic structures containing blood products of various ages. (**b**) MRI of the pelvis T1-weighted fat saturated sagittal image through the mid uterine body (same patient and level than in Fig. 3.9a): The hyperintense bloody component of the myometrial cysts makes their identification easier in T1 fat suppressed images than in T2 (Fig. 3.9a)

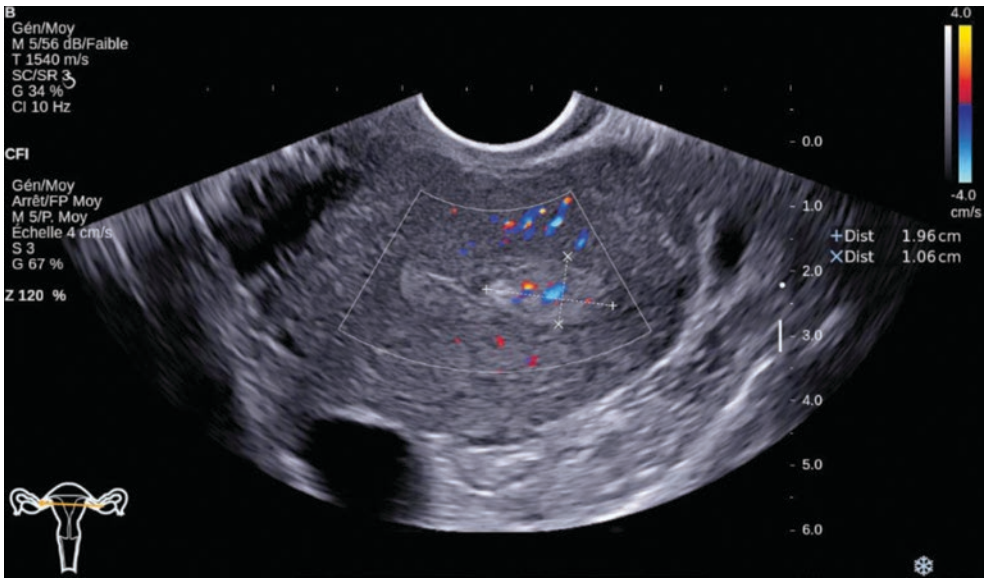

Fig. 3.10 Endovaginal ultrasound of the uterus in an axial orientation with Color Doppler shows the hyperechoic polyp with a central feeding vessel

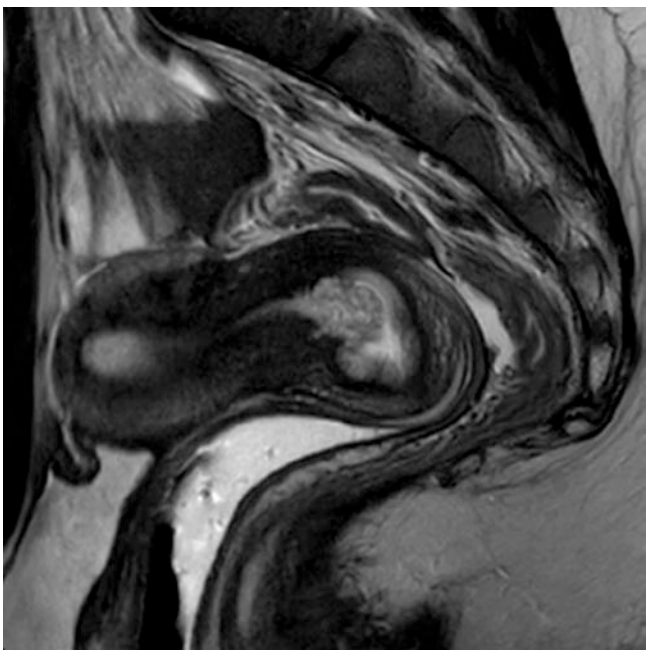

Fig. 3.11 MRI of the pelvis Sagittal T2-weighted image of the uterus with a polyp located at the internal os of the endocervical channel of a the signal intensity that is slightly hypointense compared to the normal endometrium

3.4.5 Class U4 (Hemi-uterus) (Fig. 3.6)

This anomaly is a formation defect resulting in unilateral uterine development. The contralateral part ranges from absent to incomplete formation (uterine horn remnant). U4 anomalies have two subtypes:

1. U4a (Hemi-uterus with a contralateral rudimentary (functional) cavity)—the contralateral horn has a functioning endometrial cavity that may or may not communicate with the hemi-uterus.
2. U4b (Hemi-uterus without a contralateral rudimentary (functional) cavity)—the contralateral horn is either non-functional or aplastic.

There is a high association with renal anomalies in these patients, especially renal agenesis, ipsilateral to the contralateral rudimentary horn or remnant (40%). Patients with rudimentary horns, Class U4a, require laparoscopic surgical excision. This is done to prevent hematometra and/or obstetric complications to include uterine rupture [14].

At imaging, the hemi-uterus is deviated to one side of the pelvis, and the endometrial morphology is described as "banana-" or "bullet-shaped." Uterine zonal anatomy is preserved, as is the endometrial-to-myometrial width and ratio [11]. When present, a rudimentary functional horn will have normal zonal anatomy. If it is noncommunicating, the endometrial cavity may be distended with blood, and/or there may be imaging manifestations of endometriosis. In cases without a rudimentary functional horn, the contralateral uterine horn remnant, when present, images as diffuse low to intermediate signal intensity.

3.4.6 Class U5 (Aplastic Uterus)

This anomaly is a formation defect incorporating all types of uterine aplasia. It occurs early in gestation. Affected females have no unilaterally developed or fully developed uterine cavity. U5 anomalies have two subtypes depending on

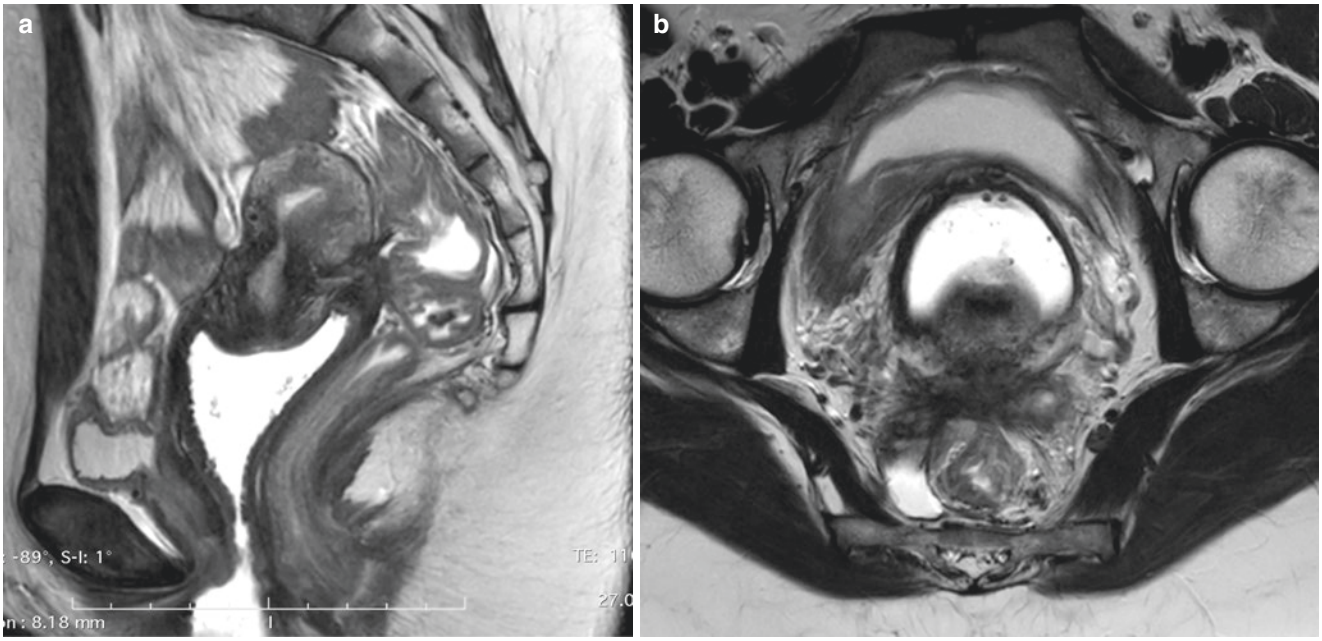

Fig. 3.12 (**a**) MRI of the pelvis Sagitall T2-weighted image through the uterine midline demonstrate a hypointense mass obliterating the posterior vaginal cuff and the retro-cervical region. Dark bandlike hypointense structures stretch towards the anterior rectal wall. (**b**) MRI of the pelvis: Corresponding axial T2-weighted image through the upper vaginal cuff shows lateral extension to both uterosacral ligaments and posterior extensions to the anterior rectal wall. Some fluid lies in the right para-rectal space delineating the posterior part of the normal distal right uterosacral ligament

whether or not there is a functional cavity in a uterine remnant if present:

1. U5a (Aplastic uterus with a rudimentary (functional) cavity)—uni- or bilateral functional uterine horn is present.
2. U5b (Aplastic uterus without rudimentary (functional) cavity)—full uterine aplasia or a non-cavitary uterine horn remnant may be present.

Cases of aplastic uterus may have coexisting defects. For example, the Mayer-Rokitansky-Küster-Hauser (MRKH) syndrome is characterized by agenesis of the vagina, cervix, and uterus.

Treatment for Class U5 patients with a rudimentary cavitary horn is not well worked out. For patients with MRKH syndrome, treatment is focused on enabling sexual function via creation of a neovagina.

On MRI, a uni- or bilateral cavitary rudimentary horn is characterized by increased T2-weighted signal intensity in the cavity, whereas a uni- or bilateral uterine horn remnant without a cavity images as diffuse low to intermediate signal intensity on T2-weighted images. For females with MRKH syndrome, fatty and connective tissue is seen in the expected location of the upper 2/3 of the vagina. No normal cervix or uterus is present. A truncated vagina may be seen between the urethra anteriorly and the rectum posteriorly.

3.4.7 Class U6 (Unclassified Cases)

A sixth class was established for cases of "infrequent anomalies, subtle changes or combined pathologies that could not be allocated correctly to one of the six groups," Classes 0–5 [8].

3.4.8 Classification of Congenital Anomalies of the Cervix and the Vagina

Coexisting anomalies of the cervix are classified from C0 to C4 according to the presence of a normal cervix (C0), a septate cervix (C1), a double "normal" cervix (C2), and a unilateral (C3) or complete cervical aplasia (C4) [8] (see Fig. 3.5). The classification of coexisting vaginal anomalies ranges from V0 (normal vagina) to V4 (vaginal aplasia) and distinguishes three types of vaginal septum: V1 is longitudinal nonobstructing, V2 longitudinal obstructing, and V3 transverse septum or imperforate hymen [8].

3.5 Leiomyoma (Figs. 3.7 and 3.8)

Ordinary leiomyomas, also called fibroid or myoma, represent benign smooth muscle tumors that can be nondegenerated or degenerated with five subcategories according to the type of degeneration (cystic, hemorrhagic, fatty, hyaline, or myxoid). The presentation at MRI shows various T2 and T1 signal intensities according to the subcategory. Variants of leiomyoma are intermediate types of leiomyoma that can be either mitotically active, cellular, atypical, or smooth muscle tumors of uncertain malignant potential (STUMP) [15]. There is currently no clinical or imaging characteristic to distinguish efficiently between ordinary leiomyoma, a very frequent gynecological tumor, and their intermediate variants. Leiomyosarcoma is an uncommon malignant smooth muscle tumor that is difficult to differentiate from ordinary leiomyoma.

On EVU leiomyomas classically represent as well-circumscribed hypoechoic masses, often associated with posterior shadowing due to calcification or at the interface with the normal myometrium. Depending on the site of development, leiomyomas are further subdivided into submucosal, intramural, or subserosal according to the FIGO classification of causes of abnormal uterine bleeding [16]. Submucosal fibroids can be either pedunculated (type 0) or of more (type 1) or less (type 2) than 50% within the cavity.

A type 3 leiomyoma contacts the endometrium. The type 4 leiomyoma is purely intramural without contact with the endometrium or the serosa.

Type 5 contacts the serosa, is subserosal, and has more than 50% intramural, and type 6 is subserosal with less than 50% intramural.

Type 7 is subserosal and pedunculated and type 8 other (e.g., cervical or broad ligament).

MRI is useful for distinguishing leiomyomas from other myometrial pathology and solid pelvic masses, especially in patients with nondiagnostic or equivocal ultrasound findings. The presence of feeding vessels originating in the myometrium further supports the uterine origin of the mass. However, if a mass is adjacent to the uterus and is of intermediate or high signal intensity relative to the myometrium on T2-weighted images, the differential diagnosis includes both degenerated leiomyoma and extrauterine tumors (benign and malignant). In these patients, the diagnosis of leiomyoma should be reserved only for cases where the uterine origin of the mass is firmly established. Occasionally, it may be difficult to distinguish a pedunculated subserosal leiomyoma from an ovarian fibroma, since both lesions may be hypointense on T2-weighted images. This distinction is likely not significant as the latter is rarely malignant.

The risk of development of a leiomyosarcoma increases with age and in black woman. The previously held view of rapid growth being at greater suspicion for sarcomas is no longer maintained as benign leiomyomas can grow rapidly and sarcomas slowly [17]. Although studies focusing on the differential diagnosis between leiomyomas and sarcomas introduce new criteria at MRI, surgical procedures have been modified because morcellation of an unsuspected leiomyosarcoma increases dissemination [18]. According to a retrospective study using MRI to differentiate 26 benign and 25 uncertain or malignant leiomyomas, the performance of MRI reached an accuracy of 92.4% using a combination of T2-weighted, B1000, and ADC features [2]. The diagnosis of malignancy could be excluded for leiomyomas that had either low (ordinary) or high T2 signal intensities (myxoid), as well as intermediate T2 and low B1000 signal intensities (cystic). For leiomyomas with intermediate T2 and high B1000, further characterization required the use of T1 signal intensities. If T1 signal intensity was high, the leiomyoma had hemorrhagic or fatty degeneration and was benign. If T1 signal intensity was low or heterogeneous, ADC values obtained at B1000 at 1.5 T were useful and only in this specific situation. A cut-off value of 0.8 was predictive of a sarcoma, above 1.2 of a benign leiomyoma, and from 0.8 to 1.2 of a leiomyoma of uncertain malignancy.

Symptomatic leiomyoma are a burden for the women affected, as well as society. In the USA, symptomatic leiomyoma remains the number one cause of hysterectomies per year and costs up to 34.4 billion dollars annually—reflecting both the direct costs of providing care to women and the indirect costs associated with lost work days and pregnancy-related issues [19]. These statistics have led to an increase in uterine-conserving therapies for affected women [20]. MRI provides a comprehensive evaluation for women who are potential uterine artery embolization (UAE) candidates. It accurately displays leiomyoma size, number, and location [21]. Additionally, in at least 20% of cases, MRI identifies autoinfarcted, comorbid, or alternative conditions that preclude UAE as primary therapy [22]. Following UAE, MRI is able to assess treatment response and identify complications such as leiomyoma delivery and pyomyoma [22–25].

3.6 Adenomyosis (Fig. 3.9)

Adenomyosis is defined as ectopic endometrial cells surrounded by stromal tissue within the myometrium and must be differentiated from leiomyoma, although these conditions frequently coexist. Differentiating the two entities may be critical because uterine-conserving therapy is established for leiomyomas, whereas hysterectomy remains the definitive treatment for debilitating adenomyosis. MRI is extremely accurate in making this distinction, especially in patients with diffuse adenomyosis with junctional zone widening >12 mm and foci of increased signal on T2-W sequences [26].

The hyperintense foci correspond to the heterotopic endometrial tissue. The surrounding muscular hyperplasia results in the low-signal myometrial lesion or widening of the junctional zone.

Hemorrhagic foci can be seen on T1-weighted sequences in approximately 20% of patients due to the presence of progesterone receptors. However, the imaging features of focal adenomyosis can overlap with those of leiomyomas [26–28]. Imaging characteristics that favor the diagnosis of focal adenomyosis include a lesion with poorly defined margins, a lesion that is elliptical in shape extending along the endometrium, a lesion that has little mass effect upon the endometrium relative to its size, and a lesion with high signal intensity striations [radiating from the endometrium into the myometrium]. Cystic adenomyosis needs to be differentiated from a leiomyoma with central hemorrhagic degeneration or a unicornuate uterus with an obstructed noncommunicating rudimentary horn.

3.7 Myometrial Contractions

Myometrial contractions can mimic leiomyoma or adenomyosis. They usually change or resolve over the course of the exam. Contractions correspond to transient low signal intensity lesions within the myometrium that deform the endometrium while sparing the outer uterine contour. Kinematic sequences using a single-shot fast spin-echo T2-weighted technique (HASTE, SSFSE) can differentiate true widening related to adenomyosis from apparent widening of the junctional zone due to myometrial contractions or uterine peristalsis, a physiologic rhythmic form of myometrial contraction most marked during the menstrual and periovulatory phase that can present as diffuse widening of the junctional zone.

3.8 Endometrial Pathology

Endometrial polyps are among the most common pathologic lesions of the uterine corpus. Patients with postmenopausal bleeding and endometrial polyps usually undergo endometrial sampling and removal of the polyps. Endometrial polyps have a variable appearance at EVS but are typically echogenic with an intact overlying endometrium or subendometrial halo. A vascular pedicle is usually identified at color/power Doppler imaging (Fig. 3.10).

Figure 3.11 MRI of the pelvis Sagittal T2-weighted images of the uterus: A polyp is located at the internal os of the endocervical canal with signal intensity that is slightly hypointense compared to normal endometrium.

Large polyps are frequently heterogeneous in signal intensity [29]. On T2-weighted sequences, the fibrous core is seen as a hypointense area within a polyp. The addition of gadolinium-enhanced sequences significantly improves the detection rate of endometrial polyps. Endometrial polyps show a variable degree of enhancement after gadolinium administration. Small polyps enhance early and are well delineated against the hypointense endometrial complex on early dynamic scans. In addition, a vascular stalk can frequently be identified during the arterial phase.

Endometrial synechia results from traumatic injury to the endometrium and may be demonstrated both with EVS and MRI. Sonohysterography improves the detection of endometrial synechiae. In severe cases of Asherman's syndrome resulting in an obliterated uterine cavity, synechiae may result in infertility, recurrent pregnancy loss, and amenorrhea. On EVS, synechiae present as echogenic or hypoechoic bands traversing the endometrial cavity. These bands can be thick and broad or thin and easily disrupted. On MRI, these bands are hypointense on T2-weighted sequences and usually show enhancement after gadolinium administration.

3.9 Benign Pathology of the Cervix and Vagina

Bartholin's cysts are caused by retained secretions within the vulvovaginal glands, mostly as a result of chronic inflammation or trauma. They are located in the posterolateral parts of the lower vagina and vulva, whereas nabothian cysts are retention cysts of the cervical glands and clefts.

Gartner duct cysts represent remnants of the caudal end of the Wolffian or mesonephric ducts and are typically located in the anterolateral wall of the vagina above the inferior margin of the symphysis pubis.

Müllerian cysts, representing embryologic remnants of Müllerian (paramesonephric) ducts, are the most common congenital cysts of the female genital tract and can be found from the introitus to the level of the cornua. They are typically lined by mucinous, columnar epithelium. At the level of the vagina, they are most commonly located anterolaterally and are indistinguishable from Gartner duct cysts. The majority of Müllerian cysts are small and asymptomatic. Large, symptomatic cysts require excision.

3.10 Deep Endometriosis

Endometriosis is a common gynecological disease, defined by functional ectopic endometrial glands and stroma outside the uterus. When located elsewhere than in the ovary or on the superficial peritoneum, endometriosis is often referred to as being deep usually lying 5 mm below the peritoneum within the bladder, vaginal, or bowel wall. Other localizations include the area behind the cervix, the upper vaginal

cuff, the ureter, the round ligament, the parameter, the uterosacral ligaments, the presacral nerves, the anterior abdominal wall, and/or the diaphragm. According to the European Society of Urogenital Radiology (ESUR), guidelines for imaging endometriosis with MRI agreed that the diagnosis of deep pelvic endometriosis requires the joint presence of morphological and signal intensity anomalies [30]: tissue areas corresponding to fibrosis with a signal close to that of pelvic muscle on T1-weighted and T2-weighted images; hyperintense foci on T1-weighted and/or fat-suppressed T1-weighted MR images, corresponding to hemorrhagic foci; and small hyperintense cavities on T2-weighted images. Morphological anomalies depend on the localization of deep endometriosis. Within the frame of this chapter, only retrocervical, uterosacral ligaments and vaginal localization are specified (Fig. 3.12a, b). Retrocervical endometriosis is also called endometriosis of the torus uterinus and corresponds at MRI to a T2 hypointense band in the upper midportion of the posterior cervix. Endometriosis of the uterosacral ligament demonstrates as an irregular nodule or thickening compared to the normal ligament. When bilateral it usually includes the torus uterinus and presents as an arciform anomaly. Vaginal endometriosis obliterates the posterior vaginal cuff with a T2 hypointense mass behind the posterior wall of the cervix. The nodule or mass may contain foci of high T2- and T1-weighted signal intensities. Vaginal endometriosis and endometriosis of the uterosacral ligaments are often associated with rectosigmoid endometriosis.

3.11 Concluding Remarks

Ultrasound is the first-line diagnostic tool for most benign uterine condition. MRI is an extremely useful complement in symptomatic patients with indeterminate or complex uterine presentation, particularly before surgery.

Take-Home Message

Ultrasound is the first-line imaging technique to localize an anomaly of the uterus to either the myometrium or the endometrium. MRI has ideal capabilities in tissue characterization and requires careful comparison between T2- and T1-weighted sequences. Image orientation perpendicular to the axis of the uterine corpus helps to assess the impact of an anomaly on the uterine cavity.

References

1. Smith-Bindman R, Kerlikowske K, Feldstein VA, et al. Endovaginal ultrasound to exclude endometrial cancer and other endometrial abnormalities. JAMA. 1998;280:1510–7.
2. Thomassin-Naggara DS, Bonneau C, et al. How to differentiate benign from malignant myometrial tumors using MR imaging. Eur Radiol. 2013;23:2306–14.
3. Troiano RN, McCarthy SM. Müllerian duct anomalies: imaging and clinical issues. Radiology. 2004;233:19–34.
4. Behr SC, Coutier JL, Qayyum A. Imaging of Müllerian Duct Anomalies. Radiographics. 2012;32:1619–20.
5. Li S, Qayyum A, Coakley FV, Hricak H. Association of renal agenesis and Müllerian duct anomalies. J Comput Assist Tomogr. 2000;24:829–34.
6. Buttram VC Jr, Gibbons WE. Müllerian anomalies: a proposed classification. (An analysis of 144 cases). Fertil Steril. 1979; 32:40–6.
7. The American Fertility Society classifications of adnexal adhesions, distal tubal occlusion, tubal occlusion secondary to tubal ligation, tubal pregnancies, Müllerian anomalies and intrauterine adhesions. Fertil Steril. 1988;49:944–55.
8. Grimbizis GF, Gordts S, Di Spiezio Sardo A, et al. The ESHRE/ESGE consensus on the classification of female genital tract congenital anomalies. Hum Reprod. 2013;28:2032–44.
9. Grimbizis GF, Di Spiezio SA, et al. The Thessaloniki ESHRE/ESGE consensus on diagnosis of female genital anomalies. Hum Reprod. 2016;31(1):2–7.
10. Mueller GC, Hussain HK, Smith YR, et al. Müllerian duct anomalies: Comparison of MRI diagnosis and clinical diagnosis. AJR Am J Roentgenol. 2007;189:1294–302.
11. Pellerito JS, McCarthy SM, Doyle MB, et al. Diagnosis of uterine anomalies: relative accuracy of MR imaging, endovaginal sonography, and hysterosalpingography. Radiology. 1992;183: 795–800.
12. Zreik TG, Troiano RN, Ghoussoub RA, et al. Myometrial tissue in uterine septa. J Am Assoc Gynecol Laparosc. 1998;5: 155–60.
13. Chandler TM, Machan LS, Cooperberg PL, et al. Müllerian duct anomalies: from diagnosis to intervention. Br J Radiol. 2009;82:1034–42.
14. Jayasinghe Y, Rane A, Stalewski H, Grover S. The presentation and early diagnosis of the rudimentary uterine horn. Obstet Gynecol. 2005;105:1456–67.
15. Arleo EK, Schwartz PE, Hui P, et al. Review of leiomyoma variants. AJR. 2015;205:912–21.
16. Munro MG, Crithcley HOD, Fraser IS, for the FIGO Working Group on Menstrual Disorders. The FIGO classification of causes of abnormal uterine bleeding. Int J Gynaecol Obstet. 2011; 113(1):1–2.
17. Peddada SD, Laughlin SK, Miner K. Growth of uterine leiomyomata among premenopausal black and white women. Proc Natl Acad Sci U S A. 2008;105(19):887–19,892.
18. FDA. UPDATED Laparoscopic Uterine Power Morcellation in Hysterectomy and Myomectomy: FDA Safety Communication 2014. Available at: http://www.fda.gov/MedicalDevices/Safety/AlertsandNotices/ucm424443.htm.
19. Cardozo ER, Clark D, Banks NK, et al. The estimated annual cost of uterine leiomyomata in the United States. Am J Obstet Gynecol. 2012;206:21.e1–9.

20. Jacobson GF, Shaber RE, Armstrong MA, Hung Y-Y. Changes in rates of hysterectomy and uterine conserving procedures for treatment of uterine leiomyoma. Am J Obstet Gynecol. 2007;196(6): 601.e1.
21. Jha RC, Ascher SM, Imaoka I, Spies JB. Symptomatic fibroleiomyomata: MR imaging of the uterus before and after uterine artery embolization. Radiology. 2000;217:228–35.
22. Nikolaidis PN, Siddiqi AH, Carr JC, et al. Incidence of nonviable leiomyomas on contrast material enhanced pelvic MR imaging in patients referred for uterine artery embolization. J Vasc Interv Radiol. 2005;16:1465–147.
23. Kroencke TJ, Scheurig C, Poellinger A, et al. Uterine artery embolization for leiomyomas: percentage of infarction predicts clinical outcome. Radiology. 2010;255:834–41.
24. Kitamura Y, Ascher SM, Cooper C, et al. Imaging manifestations of complications associated with uterine artery embolization. Radiographics. 2005;25:S119–32.
25. Radeleff B, Eiers M, Bellemann N, et al. Expulsion of dominant submucosal fibroids after uterine artery embolization. Eur J Radiol. 2010;75:e57–63.
26. Reinhold C, McCarthy S, Bret PM, et al. Diffuse adenomyosis: comparison of endovaginal US and MR imaging with histopathologic correlation. Radiology. 1996;199:151–8.
27. Togashi K, Ozasa H, Konishi I, et al. Enlarged uterus: differentiation between adenomyosis and leiomyoma with MR imaging. Radiology. 1989;171:531–4.
28. Mark AS, Hricak H, Heinrichs LW, et al. Adenomyosis and leiomyoma: differential diagnosis with MR imaging. Radiology. 1987;163:527–9.
29. Grasel RP, Outwater EK, Siegelman ES, et al. Endometrial polyps: MR imaging features and distinction from endometrial carcinoma. Radiology. 2000;214:47–52.
30. Bazot M, Bharwani N, Huchon C, et al. European society of urogenital radiology (ESUR) guidelines: MR imaging of pelvic endometriosis. Eur Radiol. 2017;27(7):2765–75.